

Performance Improvement of True Time Delay Based Centralized Beamforming Control with the Modulation Instability Phenomenon for Wireless-Array Antennas

Seyed Moin Alavi, Hassan Zakeri, Rasul Azizpour, and Gholamreza Moradi

Abstract—In this paper, we develop the performance of the modulator by using modulation instability (MI) for fifth-generation wireless communication (5G). Initially, we demonstrate how to improve the modulator’s bias voltage (V_π) with the help of carrier side-band gain due to the MI phenomenon. It’s also possible to obtain acceptable gain and bandwidth without complicating the modulator structure. In receive mode of the array antenna, where the signal is very weak, amplification in this frequency range has a critical role.

However, we present a comfortable and simple microwave-photonic beamforming bit-controller system based on the length of the fiber for receiver-transmitter phased array antennas (PAAs) that are used in high-technology wireless communication like 5G. We used the true-time delay (TTD) technique based on frequency comb to achieve beamforming of the PAA and show that the beams remain unchanged at a different frequency for different angles.

Finally, we offer the bit-control system, that the results and the benefit is illustrated by the patterns of PAA.

Index Terms—Array Antennas, Fifth-generation, Mach-Zehnder, Modulation instability, True-time-delay

I. INTRODUCTION

Microwave Photonics (MWP) is the connection between the opto-electronic and radio-frequency (RF) engineering where, in optical methods and devices, high-speed radio-frequency signals are generated, transmitted, controlled, and measured. This technique offers a large amount of processing bandwidth and provides more flexibility for information and communication technology (ICT) systems and networks. As a result, it has become widely used in a variety of applications in recent years, including wireless systems like the fifth-generation mobile communication (5G) [1], [2], optical telecommunications [3], broadband photonic signal processors [4], transceiver circuits [5], medical imaging systems using terahertz (THz) waves [6], and sensors [7].

The basic principle of MWP is that analog microwave electrical signals are transmitted through the optical fiber or photonic devices like modulators and detectors, with electrical-to-optical (EO) and optical-to-electrical (OE) transformation on the transmitting and receiving sides of the photonic link, respectively.

Seyed Moin Alavi, Hassan Zakeri, Rasul Azizpour, and Gholamreza Moradi are with the Department of Electrical Engineering, Amirkabir University of Technology (Tehran Polytechnic), Tehran, Iran (E-mails: moeinlavi@aut.ac.ir, H.Zakeri@aut.ac.ir, ra.azizpour@aut.ac.ir and, Gholmoradi@aut.ac.ir).

In biomedical applications, Gaussian pulse is used to detect and locate the exact tumor location by utilizing the modulators [8]. By reducing the pulse length by expanding bandwidth in these applications, the ability to distinguish close tumors is improved [9], which can be applied to next-generation applications that demand more precise identification and distinction.

For designing the broadband traveling-wave modulators, there are four fundamental challenges for achieving approved performance: I) matching microwave-optical velocity to avoid excitation of undesired modes on the substrate and negative effects by mismatch caused by phase velocity in optical response, II) reducing losses in microwave electrodes, III) increasing the half-wave voltage (V_π), IV) improving the impedance of the electrode (almost 50 Ω) to match better and reducing the loss of structure [10]–[12]. Using these methods make it possible to increase the modulation depth, so in this paper, we focus on reducing the V_π to improve the modulator’s response.

Theoretically, it has been shown and analyzed that the amplitude of electro-optic (EO) modulation remains stable at the sideband frequency without any losses [13]. In the experimental case, essential factors like plasmonic losses, impedance mismatching, and microwave optical velocity can decrease the signal’s modulation depth and amplitude by increasing sideband frequency. Also, the interaction between modulation voltage and arm length in EO modulators is constant and stable ($V_\pi L = \alpha$ where α is constant). Consequently, the arm length under the EO effect increases by decreasing V_π .

According to the bandwidth associated with the time constant (τ) due to the EO arm, the loss drops faster by increasing frequency, and the bandwidth decreases. So in typical cases, between V_π and bandwidth, there is a directly proportional relationship. Therefore by increasing the bandwidth, the amplitude of voltage increases too [11], [14], [15].

Decreasing mismatching between microwave-optical velocities is one of the recent methods for boosting the bandwidth range of modulator systems by keeping the V_π constant [16]. In that case, it is also possible to decrease the arm length by changing the structure of the modulator, type of excitation, and material of components.

The effective light and microwave refractive index neared each other when the plasmonic dielectric and the time constant decreased, and bandwidth rose. The complexity of a modulator increases, so the cost of the modulator structure and the range

of bandwidth is not acceptable for new applications like 5G.

Another way to achieve the same modulation depth is to use a special material with an improved EO factor. It is possible to achieve more bandwidth range and decrease the losses. Nevertheless, this method is not convenient because of the high cost of this particular material, the incompatibility of this material with the EO integrated circuits, and the low effectiveness of the EO factor [17].

In [18], another method is proposed that by using different resonators (like ring resonators) and features of the EO circuit, it is possible to create a structure with a low amplitude of V_π . These structures have more complexity than others in manufacturing the devices. Because of the deployment of the resonant feature, the modulation response fluctuates in the range of modulation depths, so the output answer is distorted.

Therefore, all of the mentioned methods can only slightly improve the V_π or bandwidth of the modulator and cannot significantly improve both parameters simultaneously, so we need to employ simple and low-cost practical applications to enhance the modulator bandwidth and V_π without altering the internal structure of the modulator.

In this paper, we propose a novel method by which it is possible to use MI phenomena in optic fiber for 5G applications in PAA in transmitting/receiving (T/R) applications.

The output to this fiber can repay the attenuation of the frequency response and reduces the required V_π of the modulator. In addition, the fiber can increase the power level in an optical link in amplifying and filtering applications [19] [20]. Increasing the gain, controlling the beamforming of the array antenna, and having a simple structure are the advantages of this method.

One of the main problems in PAAs is beam-squint, which is related to the divergence from the antenna's frequency and the structure of PAAs. Because the number of radiating elements controls the beamwidth in PAAs, a large channel number is necessary for the true-time delay (TTD) to solve the beam-squint problem and improve angular resolution.

A convenient method is proposed in [6] that replaces a single fiber and a frequency-comb source with a multiple-fiber and a single source. It is important to note that the number of frequency bands is related to the number of radiated elements. In these structures, the frequency of the difference pulses modulated on each frequency comb causes a time delay between the pulses in a fiber with a suitable dispersion. Therefore, we demonstrate that using the time delay makes it possible to increase the gain and improve the answer of the optical modulator and the bandwidth without adding any complexity to the structure. Also, we propose a new bit-controlled system that can control the directivity angle of PAA only with the length of the fiber.

The rest of the paper is organized as follows: In Section II, the MI phenomenon in optical fiber is analyzed. Section III shows the MI effect on V_π and performance enhances the intrinsically weak electro-optic development. Section IV introduces the RF and microwave TTD based on Kerr combs and their applications in PAAs. Section V shows a bit-control system based on the fiber length for controlling the beam direction of PAA.

II. FIBER UNDER MODULATION INSTABILITY

Modulation instability (MI) is a nonlinear phenomenon induced by the interaction of non-linearity, dispersion, and diffraction in the presence of an intense optical carrier wave traveling through a nonlinear medium. At the output, the exponential expansion of the spectral sidebands with the carrier wave's center band is expected. While the carrier is a CW laser optical wave, rapid fluctuations appear as modulated pulse trains [20], [21].

Because distinct spectral components are associated with the pulse travel at different speeds determined by $\frac{c}{n(w)}$, fiber dispersion is crucial in propagating short optical pulses and optical communication.

The effects of fiber dispersion are compensated for by expanding the mode-propagation constant in a Taylor series around the frequency w_0 at which the pulse spectrum is centered on accounting for the effects of fiber dispersion, that the representative equation is as follows:

$$B(w) = \sum_{m=0}^{\infty} \frac{B_m}{m!} (w - w_0)^m \quad (1)$$

The parameters $n(w)$ are group indexes, and β_1 and β_2 represent the group delay and dispersion of the group velocity, respectively.

The non-linear response of polarization to a strong optical field causes non-linear effects in optical fibers, which is another issue to consider when studying pulse propagation. The lowest-order non-linear effects in optical fibers are the third-order effects since they are constructed of silica, which has an amorphous microstructure.

Third-order non-linear phenomena in optical fibers include: The optical Kerr effect, four-wave mixing, stimulated Brillouin scattering, stimulated Raman scattering, and third-harmonic production. The optical Kerr effect has a non-linear reaction that occurs instantly and reacts to light intensity variation. When considering the propagation of strong pulses in optical fibers, both fiber dispersion and non-linearity must be regarded.

In that case, using the non-linear Schrodinger equation for optical pulse propagation as follows:

$$i \frac{\partial A}{\partial z} + i \frac{\alpha}{2} A - \frac{\beta_2}{2} \frac{\partial^2 A}{\partial T^2} + \gamma |A|^2 A = 0 \quad (2)$$

where A , γ , and α are the slowly varying envelope of the optical pulse, the non-linear parameter, and the loss factor of fiber, respectively.

Eq. (2) is easily solved to obtain the steady-state continuous radiation solution when the time derivation is ignored. In the case of the lossless response of the laser, the continuous wave for the above equation is a soliton in the form of $\sqrt{P_0} e^{i\gamma p_0 z}$ that P_0 and $\phi_{NL} = \gamma p_0 z$ are the incident power and the nonlinear phase shift induced by self-phase modulation, respectively. If the steady-state is stable against small perturbations in the power of the laser, the solution is:

$$A = (\sqrt{P_0} + a_1 e^{i(Kz - \Omega t)} + a_2 e^{-i(Kz - \Omega t)}) e^{i\gamma p_0 z} \quad (3)$$

where K is the wave number and Ω is frequency perturbation at sideband frequency of laser spectrum [20]. By replacing Eq. (3) in Eq. (2) it's possible to achieve:

$$K = \pm \frac{1}{2} |B_2 \Omega| [\Omega^2 + \text{sgn}(\beta_2) \Omega_c^2]^{\frac{1}{2}} \quad (4)$$

which Ω_c has an inverse relation with β_2 and the nonlinear length L_{NL} ($\Omega_c = 2/\sqrt{|\beta_2| L_{NL}}$). When the group velocity dispersion is positive ($\beta_2 > 0$), in all situations, the wave number (K) is real. Also, the steady state is stable in all small perturbations. On other side, when the group velocity dispersion becomes negative ($\beta_2 < 0$), the wave number is imaginary, and the perturbation increases. Therefore in the negative dispersion, the gain is:

$$g(\Omega) = |\beta_2 \Omega| \sqrt{\Omega_c^2 - \Omega^2} \quad (5)$$

The maximum gain ($g_{max}=2/L_{NL}$) also occurs at frequency $\Omega_{max} = \pm \frac{\Omega_c}{\sqrt{2}}$.

Fig. 1, shows the gain spectra for four values of the nonlinear length ($L_{NL} = 1km, 4km, 7km, 10km$) for an optical fiber with $\beta_2 = -20ps^2/km$.

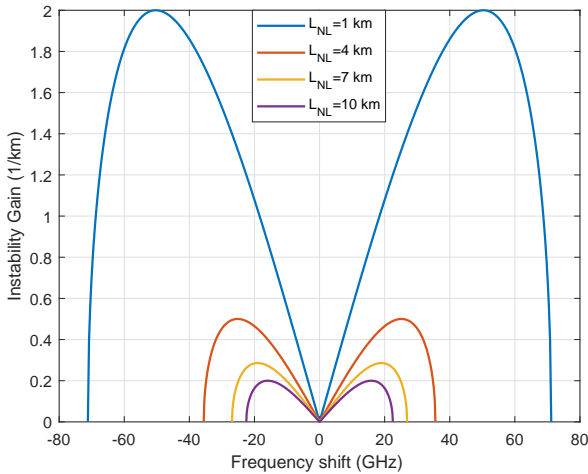


Fig. 1: Nonlinear fiber modulation instability gain diagram with the dispersion of the group velocity $\beta_2 = -20ps^2/km$ and nonlinear length $L_{NL}=1km, 4km, 7km, 10km$.

By considering frequency deviation on the laser wave, the non-linear fiber with a particular design and under modulation instability amplifies a specific spectral range of carrier sideband. Even more, it can work as a filter in this spectral range. This amplifying/filtering is applied and operated with only the anomalous fiber and does not require a separate pump [22]. Also, in some long-distance wireless applications that use an array antenna, the signal level received by the receiver is lower than the signal level detected by the receiver. An improved gain performance can maintain the antenna's high transmission capabilities. When antenna systems are required to work at mm-waves for 5G, the communication distances are drastically reduced due to the short wavelengths. Electromagnetic (EM) waves experience a higher signal quality and strength loss by atmospheric attenuations. In this case, achieving high gain is essential to reduce path loss in communication networks.

Therefore, by the introduced structure, the modulated signal can be used to be detected by the receiver.

The comparison between the power laser as input and the output of fiber under MI conditions is demonstrated in fig. 2.

It is essential to note that by the proposed structure, in which the length of fiber is $L = 11km$ and $L_{NL} = 3.23km$, the sideband level is amplified by almost 18 dBm, and also the accessible bandwidth is nearly 20 GHz, which indicates the fundamental of the role of the fiber, especially in the gain case.

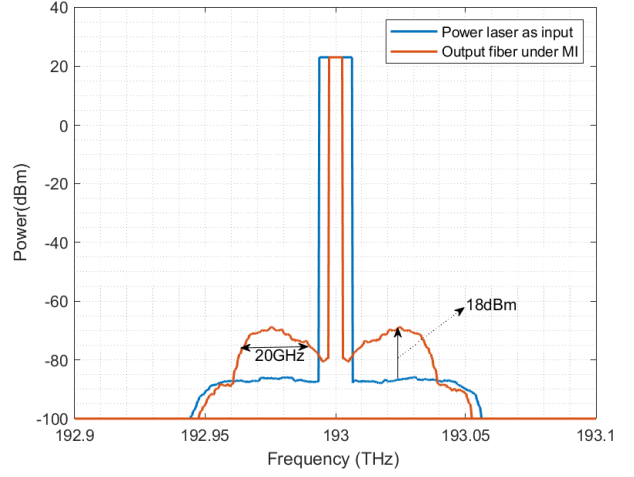


Fig. 2: Comparison between the output of fiber under MI and power laser wave as input.

III. V_π CHALLENGE IN MACH ZEHNDER MODULATOR

To design broadband traveling-wave modulators like MZ, one of the fundamental challenges to having approved performance, is raising the V_π with respect to increasing the frequency. however, in electronic devices like CMOS, this proportion is inverse [23].

The block diagram of the structure's performance of boosting output signal with fiber under MI is demonstrated in fig. 3. With the help of MZ or any similar modulator in this structure, it is possible to modulate the Gaussian pulse on the carrier. Improvement of V_π is one of the advantages of this proposed structure.

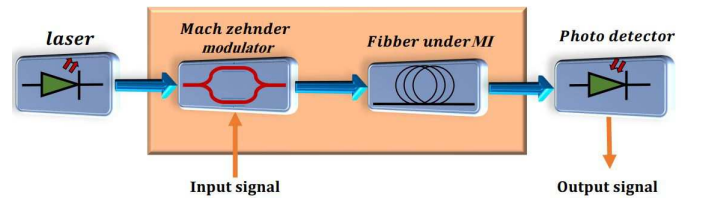


Fig. 3: Block-diagram of EO modulation structure with the fiber under the MI.

In the improved MZ modulator, the proportional relation between V_π , input/output power, and instability gain is the following:

$$P_{RF,out} \propto \frac{1}{V_\pi^2} P_{RF,in} G_{MI} \quad (6)$$

Where $P_{RF,in}(w)$, $P_{RF,out}(w)$ and G_{MI} are the input RF power, the output RF power, and modulation instability gain, respectively.

MI is stimulated by the sidebands, which results in their expansion at the expense of the carrier. The sideband fields grow by $G_{MI}^{1/2}$ as the sideband power grows by G_{MI} . The RF output power is proportional to the $G_{MI}^{1/2}$, as the measured RF current, is caused by carrier-sideband beating. The V_π necessary to obtain desirable modulation depth is decreased by using the MI in the fiber that leads the MZ modulator. The MI-induced rise of $P_{RF,out}(w)$ by G_{MI} , is similar to V_π decreasing by $G_{MI}^{1/2}$ providing the amplified modulator V_π , according to eq. 7.

$$V_{\pi,eff}(w_{RF}) = V_\pi(w_{RF}) \frac{L_{Dep}^{1/2}}{G_{MI}^{1/2}(w_{RF})} \quad (7)$$

In this equation, $L_{Dep}^{1/2} < 1$ is the consumption factor for the power carrier.

However, in transmitting and receiving communication applications, the modulator performance improves by increasing the gain that reduces the $V_{\pi,eff}$ and also helps to facilitate the detection of the received signal. It is important to note that the pulse amplification created by a fiber under MI, is spontaneous and does not need a separate amplifier or another pump. Fig. 4 shows the comparison of the V_π in the improved MZ at different non-linear lengths.

Therefore, it is possible to achieve the improvement at V_π with MI. In addition, in photonic microwave structures, the signal-to-noise ratio (SNR) is related to the inverse square of the V_π , which, due to its decrease, increases the SNR and channel capacity. With respect to the bandwidth and the amount of gain, we should design the fiber with particular parameters.

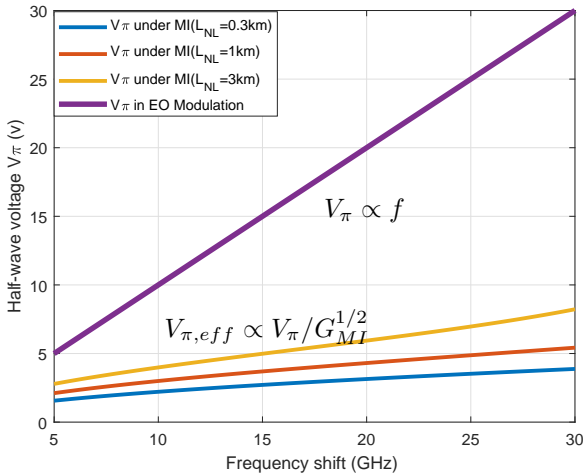


Fig. 4: Comparison of V_π between improved MZ with different L_{NL} and normal MZ.

IV. TRUE TIME DELAY IN PHASE ARRAY ANTENNA

TTD is one of the essential methods for solving beam-steering and beamforming problems in wideband PAA communication systems. Large bandwidth, immunity to electromagnetic and low loss are some of the advantages of the optical domain that it is possible to implement with the TTD.

In 5G communication wireless, beamforming can be used to offer high array gains at both the transmitter (TxBF) and receiver (RxBF), resulting in increased SNR and more radio link margin that mitigates propagation route loss. Multiple beams can be merged at the receiver to reduce path loss even more. Furthermore, interferences can be decreased, and frequency reuse can be improved using appropriate beamforming technology.

One of the simplest ways to implement TTD in MW is to use parallel and separate fibers with low dispersion. The changing of the time delay is based on the differential length between the fiber corresponding to the adjacent radiation element in PAA. However, using an individual fiber for each radiation element (multi-fiber structure) as the exciter makes the structure bulky and expensive.

A convenient method is proposed in [24] that uses a single fiber with a frequency-comb source instead of a multiple-fiber with a single source. It is important to note that the number of frequency bands is related to the number of radiated elements (M). In these types of structures, the differential frequency of modulated pulses on the adjacent frequency combs generates a time delay between the pulses in fiber with an associated dispersion.

Eq. 8 displays the relation between the TTD and the length of the fiber (L), in which D and $\Delta\lambda$ represent the fiber's dispersion and the difference between adjacent comb wavelengths, respectively.

$$\Delta\tau = DL\Delta\lambda \quad (8)$$

According to eq. 8, the theoretical value of optical true time delay (OTTD) with a relatively large free spectral range (FSR) of 200 GHz ($\Delta\lambda = 1.606$ nm) and assuming the length of fiber equivalent to 11km, is achieved as 0.136 ns. Therefore, the time delay depends on the length of the fiber, dispersion, and the frequency distance between each pulse.

$$\Theta_0 = \sin^{-1} \frac{c.mT}{d_{PAA}} \quad (9)$$

In eq. 9 it is clear that modifying the steering angle can be tuned by two methods: first, it can be accomplished by changing the FSR. Second, based the eq. 8 by changing the fiber length, and without changing the type of fiber.

In the first method, the desired frequency range is chosen from the frequency combs by using a filter. On the other hand, the second method is more practical and considered because of its facility.

In an array antenna, beamforming based on TTD has an essential role in communication systems because it shows excellent operating frequency and bandwidth performance. Low loss and immunity to electromagnetic interference are benefits that increase the quality of wireless communications.

The array antennas consist of the same and uniformly spaced radiating where θ_0 , d_{PAA} and c are radiating steering angle, spacing between each element, and speed of light in the vacuum space, respectively.

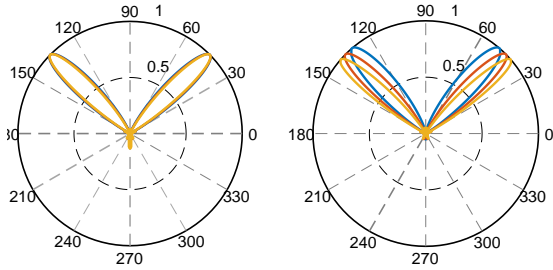


Fig. 5: Simulated beam patterns of 3 microwave frequencies with TTD-based beamformer and a phase shifter based beamformer at 42 degrees.

Fig. 5 gives us a piece of important information. Without using the TTD, the antenna's beam is dispersed and does not point to the same point. In another case with TTD, it is possible to coordinate the beam of the array antenna in the same direction in all three frequencies at 26, 28, and 31 GHz.

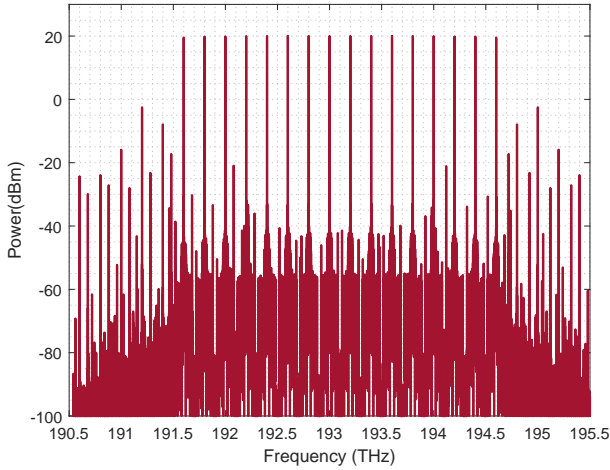


Fig. 6: Output of the frequency comb with FSR=200 GHz.

Fig. 6 shows the system response is improved due to the frequency comb source with Fsr = 200 GHz with central carrier frequency 193 THz. Also, fig. 7 demonstrates the comparison between the output of the central frequency comb and the output signal without using fiber under MI. So we can comprehend that level of the power of the output signal is increased by almost 14 dBm and the bandwidth, in that case, is 17 GHz.

V. BEAMFORMING BIT-CONTROLLER SYSTEM

Multiplexing techniques in the time, frequency, code domains, and spatial domains have been essential research areas to meet the increasing demand for spectral efficiency in fifth-generation mobile wireless communication systems. Because of its steering capability and compactness, a PAA is now

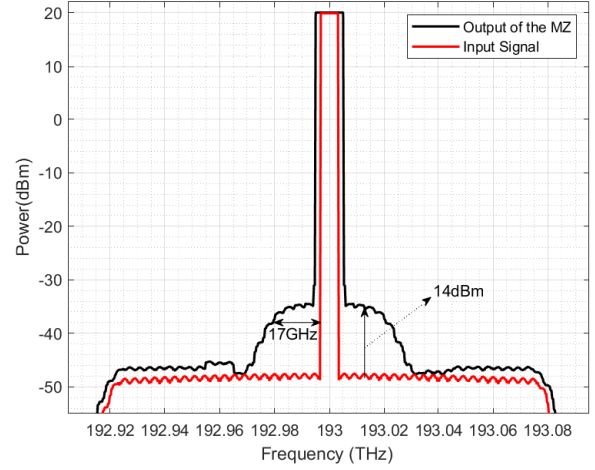


Fig. 7: Comparison of the output of the Mach-Zehnder modulator under MI phenomenon vs. without MI phenomenon.

widely utilized to achieve microwave beamforming. With a sufficient correlation between the PAA, adaptive beamforming applies to closely spaced antenna arrays. Therefore it is possible to improve network coverage, increase signal quality and exploit the array gain.

Fig. 8 demonstrates the microcomb based on a microwave TTD beamformer by arbitrary bit-control. Pumping a non-linear microresonator with a continuous wave laser produces a broadband optical frequency comb.

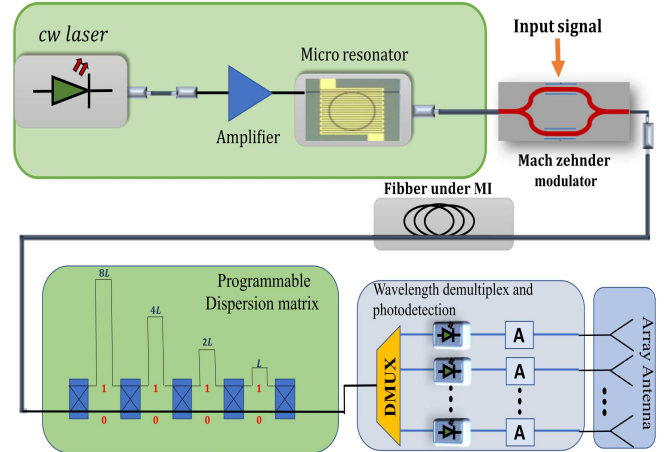


Fig. 8: Structure of modulation instability with micro comb based microwave TTD beamformer with the bit-controller-based length of the fiber.

With the help of the Mach-Zehnder, the microwave signal modulates on the frequency comb source, which is then carried by fiber under MI. Also, this fiber can boost input signals level.

A spectral shaper forms a programmable dispersion matrix in the next step. With respect to exaggerating the time delay achieved due to fiber under MI, we use a fiber with positive dispersion $\beta_2 > 0$. This elaborated solution has two benefits: first decreases the overstate time delay that is appropriate for

PAA, and second, controlling the time delay for PAA by tuning the minimum time step.

The minimum and maximum fiber lengths used in the control system are L and $15L$. To have the minimum time delay, we proposed the equation $D_1L_1 = D_2L_2$, in which D_1 and L_1 are parameters of the fiber under MI. D_2 and L_2 are the parameters of the fiber which are used in the control system. This time delay can be increased with respect to decreasing the D_2 or L_2 .

The dispersion matrix is built around a binary delay line of optical switch devices and dispersive fibers (four bits are illustrated in fig. 8).

By using the controlling system, it is possible to tune the length of the fiber, so it is available to control the time delay.

After that, the comb line is photo-detected and demultiplexed. Then the generated microwave signals are amplified and sent to an antenna array. The beam pattern can be controlled by shaping the comb spectrum with the spectral shaper, and the beam direction can be controlled by switching the dispersion matrix. Fig. 9 shows the time delay state for PAA that minimum time delay is $\Delta\tau = 1.44ps$. Therefore by changing the binary code, we can tune and control the time delay. So by changing the time delay, the beam of PAA will change.

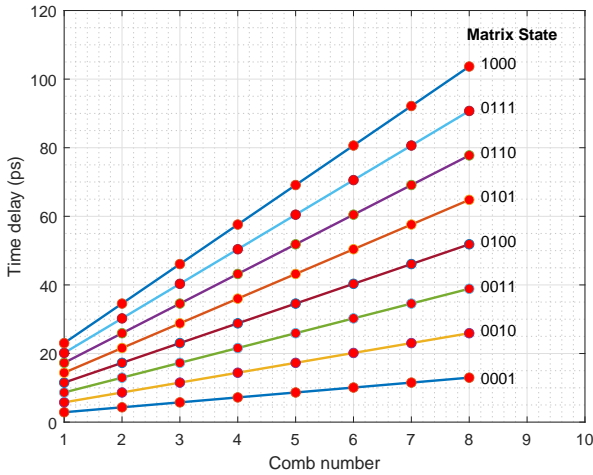


Fig. 9: Time delays of the comb lines with the dispersion matrix through the states from “0001” to “1000”.

For tuning the angle of the PAA’s main beam with the time delay between two radiating elements, we adjust the fiber length with the controlling system.

The wavelength of the laser is fixed at 1550 nm. Based on 4-bit, the target controlled fiber in the dispersion matrix is 115 m, 57.5 m, 28.75 m, and 14.375 m.

Fig. 10 (a) and fig. 10 (b) show the simulated radiation patterns for 4 and 8 array antennas for three different cases at 26, 28, and 31 GHz, respectively. The antenna’s phase offset was adjusted to direct the peak lobe at a specific angle. The distance between sub-antennas is 5.4 mm, which is half the microwave wavelength of 1.08 cm. The ω_0 represents the reference angular frequency, where the value is $2\pi \times 193$ THz.

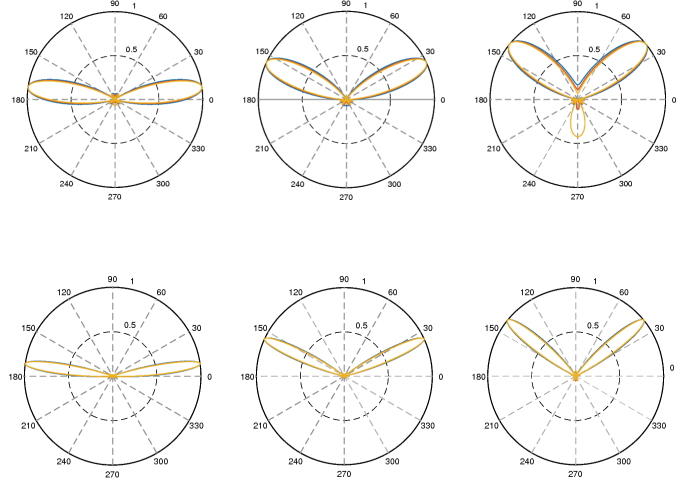


Fig. 10: Comparison of the simulated pattern at 26, 28, and 31 GHz for three different angles 8, 24, and 40 degrees.

The beam shape is Gaussian. The beam direction is 42.7 degrees, and the dispersion matrix state is “1010”. For comparison, we also calculated the beam patterns for a phase shifter controlled PAA. All the frequencies in the PAA are assumed to be the same as the 26, 28, and 31 GHz.

The rotation angle of cooperative beam-forming, which is constructed and controlled by the bits are 1101, 1001, and 0101 and with respect to the vertical axis, being nearly 8 (a), 24 (b), and 40 (c) degrees, respectively. By increasing the number of radiating elements, the pattern of the array antenna is narrow, and the effect of the back lobe decreases. So for high-technology of wireless communication, it is better to increment the number of antennas to achieve accurate results.

VI. CONCLUSION

The Mach-Zehnder modulator’s function and efficiency using MI are developed for even transmitting and receiving 5G applications. With respect to the instability gain of the carrier sideband frequency at the MI phenomenon, we demonstrate that we can improve the V_π in MZ modulator. At first, by using laser power as a carrier and the fiber under MI, we achieved 18 dBm and 20 GHz for the sideband’s gain and bandwidth, respectively.

With the help of the MZ, we modulated the frequency comb on the carrier with the central frequency 193 THz, so the gain is 14 dBm, and the bandwidth is 17 GHz. By using the fiber under MI, we increment the power of the input without adding any external device like a pump or making the structure complex.

To avoid the beam-squint, used the TTD technique to create a constant time delay for every side radiation element in PAA. In TTD, instead of employing many fibers for the excitation of PAA’s radiation element, we used a frequency comb with FSR=200 GHz. The patterns by using TTD and then comparing them without using TTD for beamforming at 26, 28, and 31 GHz frequencies are shown, respectively.

The beam is controlled with a bit-control system by using normal fiber with a length of 2.75 km. The bit-control creates

the minimum time delay=1.44 ps showing three patterns in 8, 24, and 40, degrees with respect to 1101, 1001, and 0101 binary bit-control.

REFERENCES

- [1] R. Waterhouse and D. Novack, "Realizing 5g: Microwave photonics for 5g mobile wireless systems," *IEEE Microwave Magazine*, vol. 16, no. 8, pp. 84–92, 2015.
- [2] M. Romagnoli, V. Sorianello, M. Midrio, F. H. Koppens, C. Huyghebaert, D. Neumaier, P. Galli, W. Templ, A. D'Errico, and A. C. Ferrari, "Graphene-based integrated photonics for next-generation datacom and telecom," *Nature Reviews Materials*, vol. 3, no. 10, pp. 392–414, 2018.
- [3] I. I. Nureev, O. G. Morozov, A. F. Agliyullin, V. V. Purtov, D. L. Ovchinnikov, V. I. Anfingentov, and V. Y. Vinogradov, "Microwave photonic polyharmonic probing for fiber optical telecommunication structures and measuring systems sensors monitoring," in *Optical Technologies in Telecommunications 2017*, vol. 10774. International Society for Optics and Photonics, 2018, p. 107741J.
- [4] T. Li, E. H. W. Chan, X. Wang, X. Feng, B.-O. Guan, and J. Yao, "Broadband photonic microwave signal processor with frequency up/down conversion and phase shifting capability," *IEEE Photonics Journal*, vol. 10, no. 1, pp. 1–12, 2017.
- [5] M. Chen, H. Yu, B. Yang, Y. Li, H. Chen, and S. Xie, "A silicon integrated microwave-photonic transceiver," in *2017 Optical Fiber Communications Conference and Exhibition (OFC)*. IEEE, 2017, pp. 1–3.
- [6] X. Zou, W. Bai, W. Chen, P. Li, B. Lu, G. Yu, W. Pan, B. Luo, L. Yan, and L. Shao, "Microwave photonics for featured applications in high-speed railways: communications, detection, and sensing," *Journal of Lightwave Technology*, vol. 36, no. 19, pp. 4337–4346, 2018.
- [7] J. Hervás, A. L. Ricchiuti, W. Li, N. H. Zhu, C. R. Fernández-Pousa, S. Sales, M. Li, and J. Capmany, "Microwave photonics for optical sensors," *IEEE Journal of Selected Topics in Quantum Electronics*, vol. 23, no. 2, pp. 327–339, 2017.
- [8] D. Tosi, E. Schena, C. Molardi, and S. Korganbayev, "Fiber optic sensors for sub-centimeter spatially resolved measurements: Review and biomedical applications," *Optical Fiber Technology*, vol. 43, pp. 6–19, 2018.
- [9] S. Mukherjee, L. Udpa, S. Udpa, E. J. Rothwell, and Y. Deng, "A time reversal-based microwave imaging system for detection of breast tumors," *IEEE Transactions on Microwave Theory and Techniques*, vol. 67, no. 5, pp. 2062–2075, 2019.
- [10] T. Ren, M. Zhang, C. Wang, L. Shao, C. Reimer, Y. Zhang, O. King, R. Esman, T. Cullen, and M. Lončar, "An integrated low-voltage broadband lithium niobate phase modulator," *IEEE Photonics Technology Letters*, vol. 31, no. 11, pp. 889–892, 2019.
- [11] G. K. Gopalakrishnan, W. K. Burns, R. W. McElhanon, C. H. Bulmer, and A. S. Greenblatt, "Performance and modeling of broadband linbo/sub 3/traveling wave optical intensity modulators," *Journal of Lightwave Technology*, vol. 12, no. 10, pp. 1807–1819, 1994.
- [12] D. A. Presti, V. Guarepi, F. Videla, A. Fasciszewski, and G. A. Torchia, "Intensity modulator fabricated in linbo3 by femtosecond laser writing," *Optics and Lasers in Engineering*, vol. 111, pp. 222–226, 2018.
- [13] A. Rueda, F. Sedlmeir, M. Kumari, G. Leuchs, and H. G. Schwefel, "Resonant electro-optic frequency comb," *Nature*, vol. 568, no. 7752, pp. 378–381, 2019.
- [14] J. Sun, R. Kumar, M. Sakib, J. B. Driscoll, H. Jayatilaka, and H. Rong, "A 128 gb/s pam4 silicon microring modulator with integrated thermo-optic resonance tuning," *Journal of Lightwave Technology*, vol. 37, no. 1, pp. 110–115, 2018.
- [15] Y. Sobu, T. Simoyama, S. Tanaka, Y. Tanaka, and K. Morito, "70 gbaud operation of all-silicon mach-zehnder modulator based on forward-biased pin diodes and passive equalizer," in *2019 24th OptoElectronics and Communications Conference (OECC) and 2019 International Conference on Photonics in Switching and Computing (PSC)*. IEEE, 2019, pp. 1–3.
- [16] A. Rao, A. Patil, P. Rabiei, A. Honardoost, R. DeSalvo, A. Paoletta, and S. Fathpour, "High-performance and linear thin-film lithium niobate mach-zehnder modulators on silicon up to 50 ghz," *Optics letters*, vol. 41, no. 24, pp. 5700–5703, 2016.
- [17] P. Steglich, C. Mai, D. Stolarek, S. Lischke, S. Kupijai, C. Villringer, S. Pulwer, F. Heinrich, J. Bauer, S. Meister *et al.*, "Novel ring resonator combining strong field confinement with high optical quality factor," *IEEE Photonics Technology Letters*, vol. 27, no. 20, pp. 2197–2200, 2015.
- [18] I. Demirtzioglou, C. Lacava, K. R. Bottrill, D. J. Thomson, G. T. Reed, D. J. Richardson, and P. Petropoulos, "Frequency comb generation in a silicon ring resonator modulator," *Optics express*, vol. 26, no. 2, pp. 790–796, 2018.
- [19] J. Fatome, B. Kibler, F. Leo, A. Bendahmane, G.-L. Oppo, B. Garbin, S. G. Murdoch, M. Erkintalo, and S. Coen, "Polarization modulation instability in a nonlinear fiber kerr resonator," *Optics Letters*, vol. 45, no. 18, pp. 5069–5072, 2020.
- [20] G. P. Agrawal, "Nonlinear fiber optics," in *Nonlinear Science at the Dawn of the 21st Century*. Springer, 2000, pp. 195–211.
- [21] N. A. Kudryashov, "Model of propagation pulses in an optical fiber with a new law of refractive indices," *Optik*, vol. 248, p. 168160, 2021.
- [22] P. T. DeVore, D. Borlaug, and B. Jalali, "Enhancing electrooptic modulators using modulation instability," *physica status solidi (RRL)—Rapid Research Letters*, vol. 7, no. 8, pp. 566–570, 2013.
- [23] J. Golden and D. O'Malley, "Reverse annealing for nonnegative/binary matrix factorization," *Plos one*, vol. 16, no. 1, p. e0244026, 2021.
- [24] X. Xu, J. Wu, T. G. Nguyen, T. Moein, S. T. Chu, B. E. Little, R. Morandotti, A. Mitchell, and D. J. Moss, "Photonic microwave true time delays for phased array antennas using a 49 ghz fsr integrated optical micro-comb source," *Photonics Research*, vol. 6, no. 5, pp. B30–B36, 2018.